Targeted localization of Inn1, Cyk3 and Chs2 by the mitotic-exit network regulates cytokinesis in budding yeast

Franz Meitinger[1], Boryana Petrova[1,*], Ilde Mancini Lombardi[1], Daniela Trinca Bertazzi[1], Birgit Hub[2], Hanswalter Zentgraf[2] and Gislene Pereira[1,‡]

[1]German Cancer Research Centre, DKFZ-ZMBH Alliance, Molecular Biology of Centrosomes and Cilia Unit, Im Neuenheimer Feld 581, 69120 Heidelberg, Germany
[2]German Cancer Research Centre, Department of Tumor Virology, Im Neuenheimer Feld 280, 69120 Heidelberg, Germany
*Present address: EMBL, Meyerhofstrasse 1, 69117 Heidelberg, Germany
‡Author for correspondence (g.pereira@dkfz.de)

Accepted 17 March 2010
Journal of Cell Science 123, 1851-1861

doi:10.1242/jcs.063891

Summary

The mitotic-exit network (MEN) is a signaling pathway that is essential for the coordination of mitotic exit and cytokinesis. Whereas the role of the MEN in mitotic exit is well established, the molecular mechanisms by which MEN components regulate cytokinesis remain poorly understood. Here, we show that the MEN controls components involved in septum formation, including Inn1, Cyk3 and Chs2. MEN-deficient mutants, forced to exit mitosis as a result of Cdk1 inactivation, show defects in targeting Cyk3 and Inn1 to the bud-neck region. In addition, we found that the chitin synthase Chs2 did not efficiently localize at the bud neck in the absence of MEN activity. Ultrastructural analysis of the bud neck revealed that low MEN activity led to unilateral, uncoordinated extension of the primary and secondary septa. This defect was partially suppressed by increased levels of Cyk3. We therefore propose that the MEN directly controls cytokinesis via targeting of Inn1, Cyk3 and Chs2 to the bud neck.

Key words: Cyk3, Inn1, Budding yeast, Cytokinesis, Mitotic-exit network

Introduction

Cytokinesis is a highly regulated process that leads to the physical separation of daughter and mother cell in late mitosis. Animal cells and fungi use a contractile actomyosin ring and targeted membrane addition to physically divide the cell. In animal cells, the actomyosin ring underlies the plasma membrane, and its contraction results in membrane invagination and the formation of the cleavage furrow. The fully constricted furrow is then resolved at late stages of cytokinesis by a process called abscission (Guertin et al., 2002).

Actomyosin-ring contraction is not essential for cytokinesis in budding yeast, because cells are able to survive without a contractile ring (Bi et al., 1998; Rodriguez and Paterson, 1990; Watts et al., 1987) owing to actomyosin-independent pathways that promote septum formation and/or deposition of cell-wall material at the bud neck (constriction between mother and daughter cell), which ultimately lead to separation of the two cell compartments (Balasubramanian et al., 2004; Bi, 2001). How the actomyosin-dependent and -independent pathways are regulated and coordinated at the molecular level is still largely unexplored.

In budding yeast, the initial assembly of the actomyosin ring starts early in G1 phase with the accumulation of Myo1 (the sole class-II myosin in yeast) at the bud-neck region (Bi et al., 1998; Lippincott and Li, 1998b). Additional components, including the myosin light chain Mlc1 and the conserved IQ-domain protein Iqg1, are recruited to the neck region at mid-anaphase (Epp and Chant, 1997; Shannon and Li, 1999). Just before ring contraction, actin, Hof1 (a member of the PCH family of proteins and homolog to *Schizosaccharomyces pombe* Cdc15), Cyk3 and Inn1, an essential protein required for cytokinesis, then join the ring (Korinek et al., 2000; Lippincott and Li, 1998a; Moseley and Goode, 2006; Sanchez-Diaz et al., 2008). Originally, Inn1 was reported to be involved in coordinating actomyosin-ring contraction with membrane ingression (Sanchez-Diaz et al., 2008); a later study, however, showed that Inn1, Hof1 and Cyk3 form a complex that is likely to be involved in formation of the primary septum (Nishihama et al., 2009). The primary septum is a chitin-rich layer of the cell wall and is uniformly deposited by chitin synthase 2 (Chs2), an enzyme delivered to the bud-neck region by targeted membrane trafficking (Chuang and Schekman, 1996; Sburlati and Cabib, 1986; Zhang et al., 2006). After completion of the primary septum, the secondary septum is deposited on both sides of the primary septum. The secondary septum contains mannan and glucan, and is thus more similar to the rest of the cell wall (Cabib et al., 1982). At a later stage, chitinase and other enzymes allow the complete separation between mother and daughter cell by partially hydrolyzing the primary septum (Cabib, 2004).

Cytokinesis must also be temporally coordinated with other mitotic processes to ensure that it occurs after chromosome segregation. As cells enter mitosis, the activity of the mitotic cyclin-dependent kinase Cdk1 increases to promote spindle assembly and partitioning of sister chromatids. Budding yeast contains one single gene encoding Cdk1, named *CDC28* (Nasmyth, 1993). For cells to physically divide and also to start a new round of DNA replication, mitotic Cdk1 activity must be downregulated. In budding yeast, a GTPase-driven signaling cascade named the mitotic-exit network (MEN) drives exit from mitosis. Activation of the MEN occurs once one set of sister chromatids is delivered together with the spindle pole body (SPB) into the daughter cell.

Journal of Cell Science

The SPB is the functional equivalent of the mammalian centrosome. Activation of the MEN ultimately promotes mitotic Cdk1 inactivation and thus indirectly triggers cytokinesis (Bardin and Amon, 2001).

MEN components consist of the Ras-like GTPase Tem1, the kinases Cdc5, Cdc15 and Dbf2 (and its paralog, Dbf20), and the Dbf2 and Dbf20 (Dbf2/20) regulatory protein Mob1. Most MEN components localize at the SPBs, in which the Tem1-specific GTPase-activating protein (GAP) complex keeps Tem1 inactive until the SPB enters the daughter cell (Pereira and Schiebel, 2001). The MEN promotes activation of the phosphatase Cdc14, which in turn leads to Cdk1 inactivation, spindle disassembly and ultimately cytokinesis through dephosphorylation of key mitotic Cdk1 targets (Stegmeier and Amon, 2004).

There is, however, mounting evidence pointing towards a more direct role of the MEN in cytokinesis. As the activity of mitotic Cdk1 drops, the MEN components Cdc15, Dbf2/20 and Mob1, the MEN regulator Cdc5 and the MEN target Cdc14 associate with the bud neck (Bembenek et al., 2005; Frenz et al., 2000; Luca et al., 2001; Song et al., 2000; Xu et al., 2000). Cells in which MEN proteins are not functional but mitotic Cdk1 is ectopically inactivated show defects in actomyosin-ring contraction, actin repolarization and cell separation (Corbett et al., 2006; Hwa Lim et al., 2003; Yeong, 2005; Yeong et al., 2002). Recently, Cdc5, but not other MEN kinases, was shown to promote actomyosin-ring formation via activation of the conserved GTPase Rho1 (Yoshida et al., 2006). However, it is still unclear whether the MEN controls only the contraction of the actomyosin ring or whether it promotes cytokinesis also through regulation of actomyosin-independent pathways.

In this study, we systematically analyzed the contribution of the MEN in the actomyosin-independent pathway. We show that MEN mutants are unable to grow in the absence of the actomyosin-ring component Myo1. Under conditions of low Cdk1 activity, inactivation of the MEN kinases Dbf2 and Dbf20 causes disorganized formation of the primary and secondary septa. Furthermore, the MEN is required for proper localization of Cyk3, Chs2 and Inn1 to the bud neck. We propose that, during mitotic exit, MEN activity is required to target proteins that function in actomyosin-ring-independent pathways of septum formation to the bud neck.

Results

MEN is involved in both actomyosin-ring-dependent and -independent cytokinetic pathways

Functional characterization of cytokinetic components in budding yeast is often complicated by the fact that several pathways contribute to cytokinesis. For example, deletion of *MYO1* is not lethal when components involved in primary- and secondary-septa formation are present (Bi et al., 1998). Consequently, deletion of genes involved in septum formation leads to lethality in *myo1Δ* cells. On the basis of such synthetic lethal interactions, three genetic pathways that contribute to cytokinesis have been defined (Fig. 1A). Myo1 belongs to the actomyosin-ring-dependent pathway, whereas Hof1 and Cyk3 participate in actomyosin-independent processes involved in septum formation (Korinek et al., 2000; Vallen et al., 2000). In order to get a better insight into the nature of the cytokinetic events that depend on MEN activity, we systematically assessed the effects of MEN loss-of-function mutations in cells simultaneously deficient for *MYO1*, *CYK3* and *HOF1*. In addition, we included *INN1*, the gene product of which was recently reported to complex with Hof1 and Cyk3 and localize at the bud neck in late telophase (Nishihama et al., 2009; Sanchez-Diaz et al., 2008).

In agreement with previous studies (Korinek et al., 2000; Vallen et al., 2000), cells individually deficient for *MYO1*, *CYK3* or *HOF1* were viable in our strain background (Fig. 1B, lanes 2, 5, 8), whereas *myo1Δ hof1Δ*, *myo1Δ cyk3Δ* and *hof1Δ cyk3Δ* double knockouts were not (data not shown). Because deletion of *INN1* alone was lethal, we constructed *INN1* temperature-sensitive mutant (*inn1-ts*) using the *inn1-ts* allele recently described (Ben-Aroya et al., 2008). Cells carrying *inn1-ts* were viable at 23°C but unable to grow when also deficient for *HOF1*, *CYK3* or *MYO1* (Fig. 1B, lanes 1, 4 and 7). Thus, *INN1* interacts genetically with genes involved in different steps of cytokinesis (Fig. 1A), indicating overlapping functions.

We then assessed the requirement of *MYO1*, *HOF1*, *CYK3* and *INN1* for the survival of MEN mutants (Fig. 1C). Deletion of *MYO1* was lethal in *tem1-3*, *cdc15-1*, *dbf2-2* and *mob1-67* cells (Fig. 1C, lanes 8, 10, 14 and 17), and greatly impaired the growth of *cdc5-10* and *cdc14-2* cells (not shown). Morphological examination of MEN mutants lacking *MYO1* revealed an increased accumulation of budded cells of abnormally larger size in addition to chains of interconnected cells, phenotypes indicative of cytokinesis defects. Thus, cells with compromised MEN activity are unable to complete cytokinesis in the absence of *MYO1* (actomyosin-ring formation). Mutations in MEN components also compromised cell viability when combined with *HOF1* and *CYK3* deletions (Fig. 1C, lanes 6, 7, 12, 13, 16, 19). In addition, *inn1-ts* cells were inviable in the *mob1-67* background (Fig. 1D, lane 5) and grew extremely poorly when combined with *dbf2-2 dbf20Δ* mutations (Fig. 1D, lane 7). Together, this genetic analysis suggests that MEN activity (directly or via Cdk1 inactivation) is important for the normal function or regulation of multiple cytokinetic pathways.

The binding of Inn1 and Hof1 to the bud neck is under the control of Cdk1 activity

To further investigate this hypothesis, we analyzed the effect of MEN inactivation upon localization of the components Hof1, Inn1 and Cyk3. Because MEN is required to trigger the downregulation of mitotic Cdk1 in late mitosis, defects in MEN activation will indirectly impair cytokinesis (Surana et al., 1993). To circumvent this problem, we analyzed the phenotype of MEN mutants carrying a non-phosphorylatable form of the Cdk1 inhibitor Sic1 (*SIC1*^{T5V,T33V,S76A}; hereafter referred to as *SIC1*^{S} for Sic1-stabilized) under the control of an inducible promoter (Gal1), which leads to accumulation of Sic1^{S} and mitotic Cdk1 inhibition upon promoter activation (Schwob et al., 1994).

Hof1 associates with septins throughout most phases of the cell cycle and merges with the actomyosin single ring in late mitosis (Kamei et al., 1998; Lippincott and Li, 1998a; Vallen et al., 2000). Interestingly, Hof1 does not bind to the actomyosin ring in MEN mutants (Kamei et al., 1998; Lippincott and Li, 1998a; Vallen et al., 2000), raising the question of whether MEN regulates Hof1 localization directly or indirectly (via Cdk1 inactivation). To address this, Hof1-GFP localization was monitored in wild-type Gal1-*SIC1*^{S} and *dbf2-2 dbf20Δ* Gal1-*SIC1*^{S} cells that were incubated at 37°C, to inactivate Dbf2-2 kinase activity, prior to ectopic inactivation of Cdk1 through *SIC1*^{S} overexpression. Cells also carried *MYO1-eqFP* (Wiedenmann et al., 2002) to allow visualization of the actomyosin ring. In both wild-type and *dbf2-2*

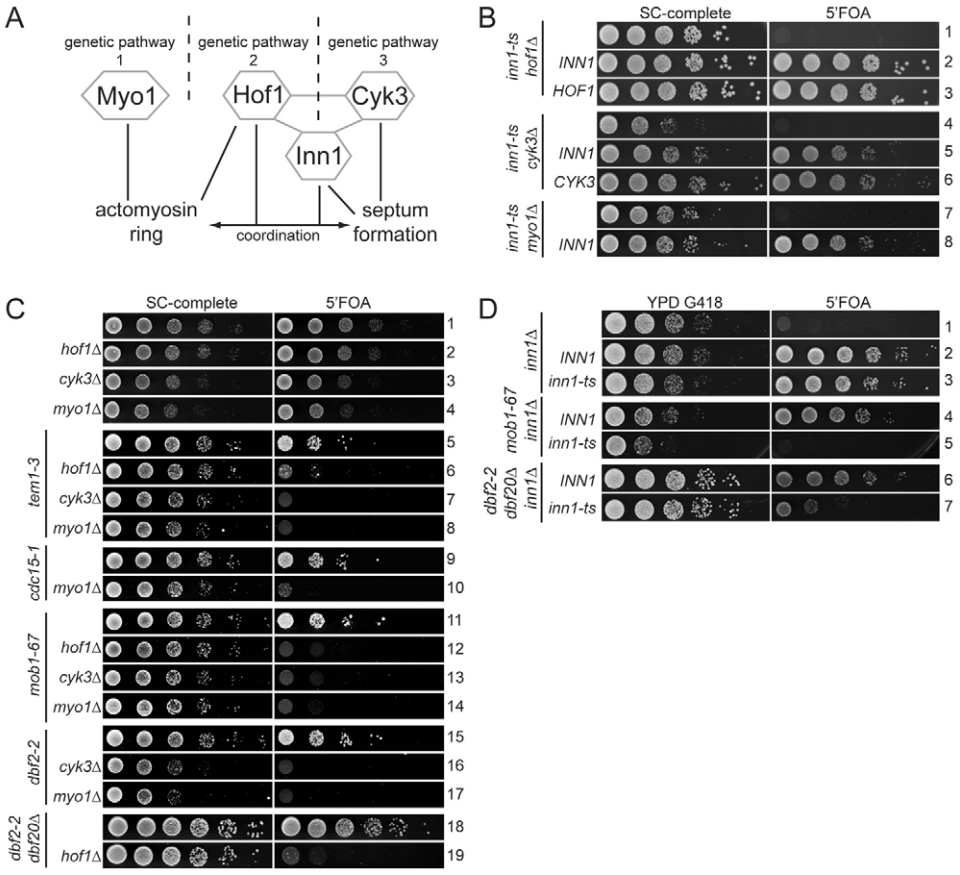

Fig. 1. Genetic interaction between MEN mutants and genes involved in cytokinesis. (**A**) Schematic representation of the genetic pathways involving *MYO1*, *HOF1* and *CYK3* during cytokinesis (see text for details). (**B**) *HOF1*, *CYK3* and *MYO1* were deleted in *inn1-ts* cells carrying wild-type *INN1* on a *URA3*-based plasmid (lanes 1, 4, 7). Tenfold serial dilutions of the indicated strains were spotted on SC-complete and 5′FOA plates, and the cell growth was inspected after 3 days at 23°C. *INN1* (lanes 2, 5, 8), *HOF1* (lane 3) and *CYK3* (lane 6) on *LEU2*-based plasmids were able to complement the growth of the corresponding double mutants. (**C**) Tenfold serial dilutions of wild-type cells (YPH499) and MEN mutants carrying *hof1Δ*, *cyk3Δ* or *myo1Δ* (complemented with the appropriate wild-type gene on a *URA3*-based plasmid) were spotted onto SC-complete and 5′FOA plates. Plates were incubated for 3 days at 23°C. (**D**) *INN1* was deleted in the indicated MEN mutants, which were kept alive by a *URA3*-based plasmid carrying *INN1*. Cell growth was tested on YPD-G418 and 5′FOA plates at 23°C after transformation with G418-based plasmids carrying *INN1* or *inn1-ts*.

dbf20Δ cells, Hof1 appeared in metaphase as a double ring owing to its association with septins and it colocalized with Myo1-eqFP as soon as cells progressed into anaphase (supplementary material Fig. S1). Similar results were observed for *tem1-3*, *cdc15-1*, *mob1-67* and *cdc14-2* Gal1-*SIC1*^{S} mutants (data not shown). Thus, Cdk1 inactivation is sufficient to permit association of Hof1 with the actomyosin ring independently of MEN activity.

To define how Inn1 localization is regulated with respect to cell-cycle progression and whether MEN is directly involved in this process, we first defined the precise timing of localization of Inn1 to the bud neck in comparison with Clb2 degradation and Sic1 accumulation (markers of mitotic exit) in wild-type cells using C-terminal fusions of *INN1* with *GFP* or monomeric *CHERRY* (Maeder et al., 2007) at the *INN1* locus. Inn1-GFP localized to the bud neck during late mitosis concomitantly with decreasing Clb2 and increasing Sic1 levels (supplementary material Fig. S2A). Association of Inn1 with the bud neck was very transient (4-5 minutes; n=10) and occurred 3-4 minutes prior to spindle disassembly and 1-2 minutes before the onset of actomyosin-ring contraction (supplementary material Fig. S2B,C). In temperature-sensitive MEN mutants or cells overexpressing a non-degradable form of *CLB2* (*CLB2ΔDB*) (Surana et al., 1993), Inn1-GFP accumulation at the bud neck was greatly reduced (supplementary material Fig. S3). This result indicates that Inn1 bud-neck localization is dependent upon Cdk1 inactivation, which is in line with a recent publication (Nishihama et al., 2009).

We next analyzed whether MEN components are directly involved in controlling Inn1 bud-neck localization. For this, we ectopically expressed the Cdk1 inhibitor *SIC1*^{S} in wild-type and MEN-deficient cells that were previously arrested in metaphase (Fig. 2). In MEN mutants, actin fails to repolarize to the bud-neck region because of high Cdk1 activity (Lew and Reed, 1993; Moseley and Goode, 2006). Overexpression of *SIC1*^{S} restored actin repolarization, indicating that a significant drop in Cdk1 activity was achieved in the absence of a functional MEN (Fig. 2). In wild-type cells, Inn1 accumulated at the bud neck proportionally to the appearance of anaphase cells with or without *SIC1*^{S} expression (Fig. 2A,B). In *dbf2-2* mutants, Inn1 failed to accumulate at the bud neck in most of the cells (>90%). Only very weak Inn1-GFP ring or dot-like staining could be observed in 5-10% of *dbf2-2* anaphase cells after prolonged incubations (Fig. 2C). By contrast, Inn1 efficiently accumulated at the bud neck upon Sic1^{S} overproduction in *dbf2-2* cells (Fig. 2D). Ring and dot-like signals were observed in addition to split dot foci, which accumulated at later time points (Fig. 2D, split dots). The latter phenotype might be a consequence of persistent association of Inn1-GFP with the actomyosin ring, which fails to contract in MEN mutants forced to exit mitosis (supplementary material Fig. S1D). Similar results were obtained for *tem1-3*, *cdc15-1*, *mob1-67* and *cdc14-2* Gal1-*SIC1*^{S} cells (data not shown). Finally, we established that inactivation of Cdk1 using the ATP analog 1NM-PP1 (Bishop et al., 2000) to specifically inhibit the kinase activity of the Cdk1-analog-sensitive (Cdk1-as1) protein also resulted in rapid accumulation of Inn1 at the neck in *cdk1-as1 dbf2-2 dbf20Δ* cells (Fig. 2E,F). Collectively, these data show that mitotic Cdk1 inactivation is sufficient to trigger Inn1 and Hof1 localization to the actomyosin ring in the absence of MEN activity.

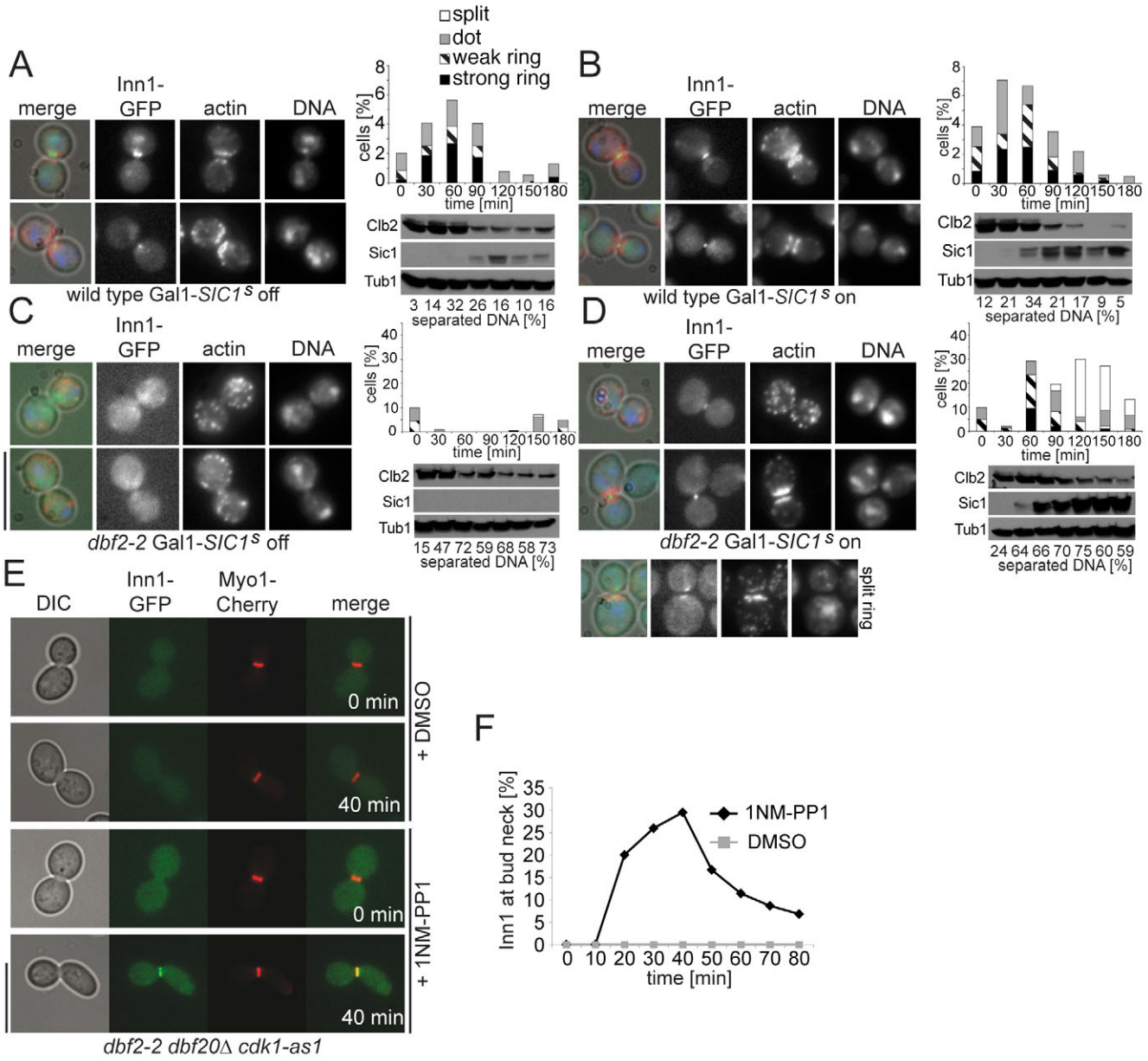

Fig. 2. Localization of Inn1-GFP in MEN mutants. (**A-D**) Inn1 localization at the bud neck in MEN mutants upon mitotic exit. The indicated cell types carrying Gal1-*SIC1*^{S} were arrested in metaphase at 23°C followed by a shift to 37°C for 30 minutes. The metaphase block was released by washing with nocodazole-free medium containing 2% glucose (no *SIC1*^{S} expression; A,C) or 2% galactose to induce *SIC1*^{S} expression (B,D). Samples were taken at the indicated time points and fixed for Inn1-GFP, Rhodamine-phalloidin (actin labeling) and DAPI (DNA). Inn1-GFP at the bud neck was scored as weak ring, strong ring, dot and split dot-like signals (representative staining for split dots is shown in D; 100-150 cells were scored for each time point). Amounts of Clb2 and Sic1 were analyzed by immunoblots. Tub1 served as a loading control. (**E**,**F**) Localization of Inn1 at the bud neck upon Cdk1 inhibition. *INN1-GFP MYO1-CHERRY dbf2-2 dbf20Δ* cells carrying the ATP-analog-sensitive *cdk1-as1* allele were arrested in late anaphase by incubation at 37°C. Inn1-GFP and Myo1-Cherry were monitored after 1NM-PP1 or DMSO (solvent control) addition (n=100 per time point). Scale bars: 10 μm.

MEN is needed for bud-neck association of Inn1 in cells lacking *HOF1*

To better understand the mechanisms that regulate Inn1 localization, we next analyzed the relative timing of Inn1 and Hof1 binding to the bud neck using *INN1-GFP HOF1-CHERRY* cells. In wild-type cells, Inn1 and Hof1 bound to the actomyosin ring with similar timing (supplementary material Fig. S4A, B). This might suggest that Inn1 binds to the bud neck via Hof1. However, in *hof1Δ* cells, Inn1 still localized at the actomyosin ring with kinetics similar to wild-type cells (supplementary material Fig. S4C). Moreover, deletion of *CYK3* had also no influence on Inn1 bud-neck localization (data not shown). Thus, individual deletion of either *HOF1* or *CYK3* did not influence the timing of Inn1 bud-neck association. We could not probe the effect of double deletions, because we were unable to obtain viable *hof1Δ cyk3Δ* mutants in our strain background using repressible promoters.

We next investigated whether MEN is required to target Inn1 to the bud neck in the absence of *HOF1* or *CYK3*. Most MEN

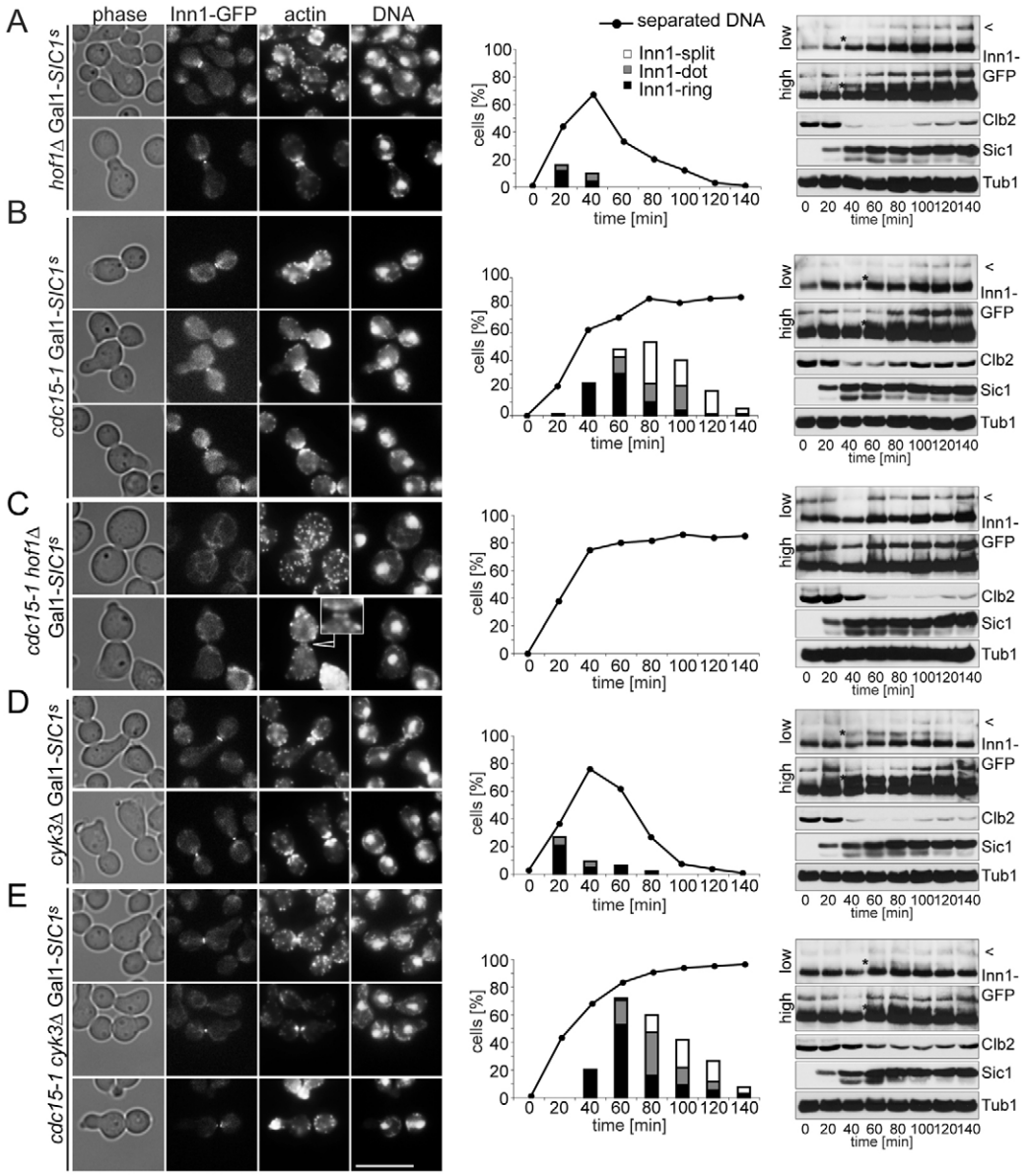

Fig. 3. MEN and Hof1 are involved in Inn1 localization. (**A-E**) The indicated cell types carrying *INN1-GFP* were arrested with α-factor at 23°C (G1-phase block). Cells were released at 37°C in nocodazole-containing medium (metaphase arrest, *t*=0) to inactivate Cdc15-1 kinase activity. Cells were allowed to progress into anaphase at 37°C by washing out nocodazole in medium containing galactose (to induce Gal1-*SIC1*^{S} expression). Cell-cycle progression, Inn1-GFP localization and actin (Rhodamine-phalloidin staining) were monitored over time. DNA was stained with DAPI. The inset in C shows an actin ring at the bud neck (marked by the arrowhead). The graphs represent the quantification of Inn1-GFP signal and the percentage of cells with separated DNA masses (100-150 cells were scored per time point). Inn1-GFP, Clb2 and Sic1 protein levels were investigated by immunoblot. Tub1 served as a loading control. Two exposures times (low and high) are shown for Inn1-GFP blots. The arrowheads indicate an unspecific cross-reaction protein band and asterisks mark the slow-migrating, phosphorylated forms of Inn1. Scale bars: 10 μm.

mutants are synthetically lethal with deletions of *HOF1* or *CYK3* (Fig. 1). However, *cdc15-1* and *cdc14-2* cells were viable in the absence of *HOF1* or *CYK3*, despite growth defects of the double mutants. We therefore analyzed the localization of Inn1-GFP in *cdc15-1* Gal1-*SIC1*^{S} *hof1Δ* and *cdc15-1* Gal1-*SIC1*^{S} *cyk3Δ* cells upon MEN and Cdk1 inactivation (Fig. 3). Inn1-GFP localized to the bud neck with similar kinetics in Gal1-*SIC1*^{S}, *hof1Δ* Gal1-*SIC1*^{S}, *cdc15-1* Gal1-*SIC1*^{S} and *cdc15-1 cyk3Δ* Gal1-*SIC1*^{S} cells (Fig. 3A,B,D,E and data not shown). Uniquely, however, Inn1 completely failed to localize to the bud-neck region upon inactivation of both MEN and Cdk1 in *cdc15-1 hof1Δ* Gal1-*SIC1*^{S} cells (Fig. 3C). The impaired Inn1-GFP localization, in the absence of *HOF1*, was not due to reduced amount of Inn1 protein, because the steady-state levels of Inn1-GFP were similar in all cell backgrounds (Fig. 3).

Interestingly, repolarization of actin to the bud neck was not observed in *cdc15-1 hof1Δ* Gal1-*SIC1*^{S} cells (upon Cdk1 downregulation), whereas it occurred in cells with *hof1Δ*, *cyk3Δ*, *cdc15-1* and *cdc15-1 cyk3Δ* with Gal1-*SIC1*^{S} (Fig. 3). An F-actin ring was, however, observed in *cdc15-1 hof1Δ* Gal1-*SIC1*^{S} cells

(Fig. 3C, inset). This shows that *cdc15-1 hof1Δ* cells are only defective in actin patch repolarization but not in F-actin ring assembly. The same results were obtained for *cdc14-2 hof1Δ Gal1-SIC1^S* cells (data not shown). Thus, inactivation of Cdk1 is only sufficient to target Inn1 to the bud neck when either the MEN or Hof1 is functional. It is possible that the failed organization of the actin cytoskeleton in *cdc15-1 hof1Δ* cells plays a role in Inn1 bud-neck targeting, because actin depolymerization causes the same phenotype in *hof1Δ* cells (Nishihama et al., 2009).

Inn1 has been reported to be subject to cell-cycle-dependent phosphorylation (Nishihama et al., 2009). Intriguingly, whereas hyperphosphorylated forms of Inn1 (Fig. 3A,B,D,E, asterisks) were present in Gal1-*SIC1^S*-overexpressing wild-type, *cdc15-1* and *cdc15-1 cyk3Δ* cells, only the non-phosphorylated faster-migrating form of Inn1-GFP was observed in *cdc15-1* Gal1-*SIC1^S* cells lacking *HOF1* (Fig. 3C). Thus, hyperphosphorylation of Inn1 seems to correlate with its association with the bud neck. In conclusion, upon mitotic exit, Inn1 bud-neck localization in wild-type yeast cells is dependent on both the MEN and Hof1.

MEN activity is required for the localization of Cyk3 to the bud neck

Because Inn1 interacts with Hof1 and Cyk3, we next investigated the importance of mitotic-exit events for Cyk3 bud-neck localization. High mitotic Cdk1 activity inhibited the localization of Cyk3 at the bud neck: Cyk3-GFP failed to accumulate at the neck region in MEN mutants and in cells overexpressing the non-degradable form of the mitotic cyclin (Fig. 4 and data not shown). Interestingly, ectopic inactivation of Cdk1 was not able to restore bud-neck localization of Cyk3-GFP in *dbf2-2 dbf20Δ* Gal1-*SIC1^S* cells (Fig. 4A-C, 30 minutes). After prolonged *SIC1^S* overexpression (75-90 minutes), Cyk3-GFP could only be detected at the bud neck in a small percentage of *dbf2-2 dbf20Δ* cells (Fig. 4A, 75 minutes and Fig. 4C). However, this Cyk3-GFP signal was much weaker in comparison to the signal obtained in wild-type cells (Fig. 4D). We also established that Cyk3 protein levels were not reduced in *dbf2-2 dbf20Δ* Gal1-*SIC1^S* cells (Fig. 4E). To confirm that MEN is directly involved in Cyk3 localization, we analyzed *cdk1-as1 dbf2-2 dbf20Δ* cells expressing *INN1-GFP CYK3-CHERRY* (Fig. 4F-H). In cycling cells in the absence of the Cdk1 inhibitor, Inn1-GFP and Cyk3-Cherry colocalized at the bud

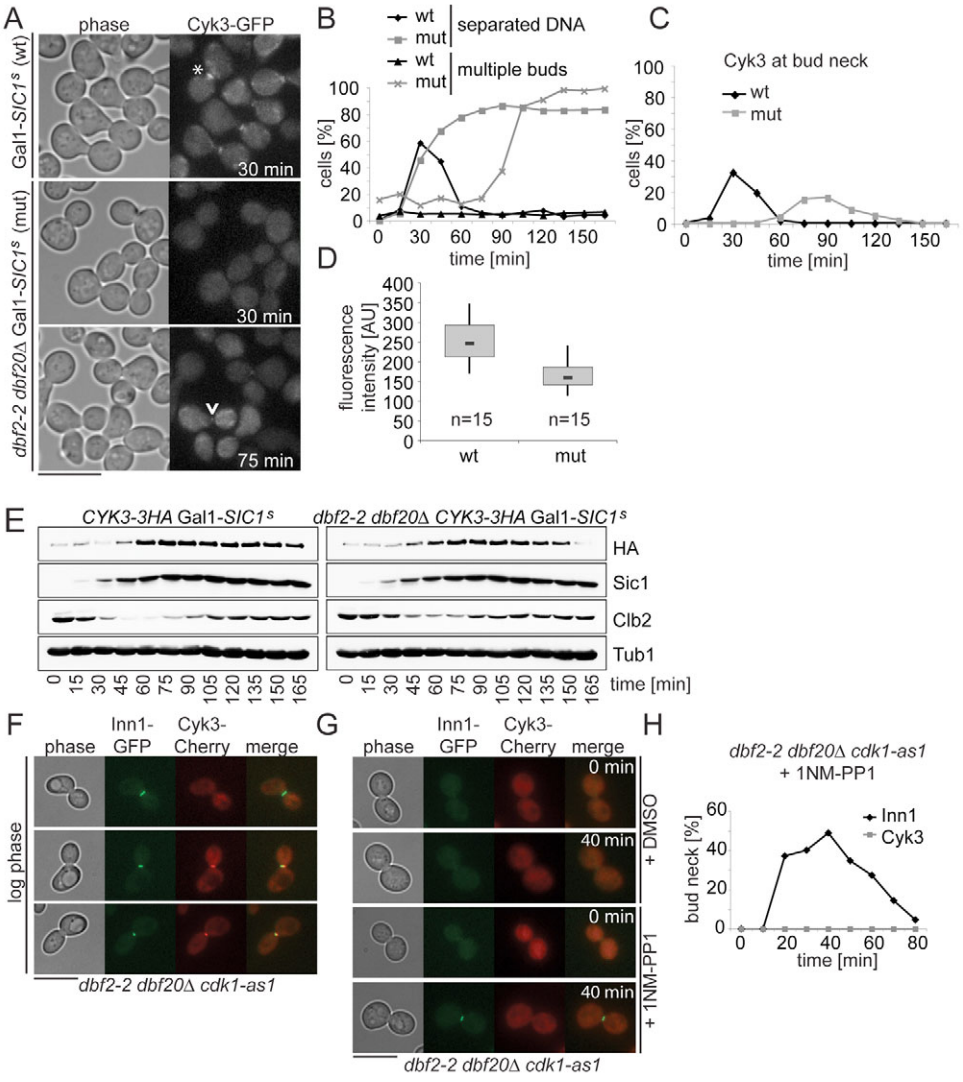

Fig. 4. Cyk3 localization at the bud neck depends on MEN. (A-D) Cyk3-GFP bud-neck localization. (**A**) The indicated cell types carrying *CYK3-GFP* were treated as in Fig. 3. Cyk3-GFP localization was monitored over time. Cyk3-GFP ring staining in Gal1-*SIC1^S* (wt, asterisk) and *dbf2-2 dbf20Δ* Gal1-*SIC1^S* (mut, arrowhead) cells are indicated. (**B**) Separation of the DNA masses and appearance of multiple budded cells were scored over time. (**C**) Percentage of cells with Cyk3-GFP signal at the bud neck. In B and C, 100 cells were scored per time point. (**D**) Quantification of the Cyk3-GFP bud-neck signals of A in arbitrary units. (**E**) *CYK3-3HA*-expressing cells were treated as in A. Cyk3-3HA, Clb2 and Sic1 protein levels were monitored by immunoblot. Tub1 served as a loading control. (**F**) Inn1-GFP and Cyk3-Cherry colocalize at the bud neck in logarithmically growing *dbf2-2 dbf20Δ cdk1-as1* cells. (**G**,**H**) Cyk3 bud-neck localization is compromised in *dbf2-2 dbf20Δ* cells upon Cdk1-as1 inhibition. Cells of *dbf2-2 dbf20Δ cdk1-as1* were arrested in late anaphase at 37°C for 3-4 hours. DMSO (control) or 1NM-PP1 was added to the cultures. Inn1-GFP and Cyk3-Cherry colocalization was monitored over time. (H) Quantification of G (*n*=100 per time point). Scale bars: 10 μm.

neck in late mitosis with very similar kinetics. In a small percentage of cells (5-10%), Inn1-GFP localization preceded that of Cyk3-Cherry, implying that Cyk3 might bind shortly after Inn1 at the bud neck (Fig. 4F, upper panel). In *cdk1-as1 dbf2-2 dbf20Δ* cells that were arrested in late anaphase by incubation at 37°C, neither Inn1 nor Cyk3 localized at the bud neck (Fig. 4G,H, 0 minutes). Upon Cdk1-as1 inactivation using the inhibitor 1NM-PP1, Inn1-GFP bud-neck localization was restored; however, Cyk3-Cherry completely failed to bind to the bud neck (Fig. 4G-H). Dbf2/Dbf20 activities are therefore crucial to bring Cyk3 to the bud neck in late anaphase in the presence of low Cdk1 activity.

Because Cyk3 forms a complex with Inn1 and Hof1, we also investigated whether Hof1 and Inn1 are required for the binding of Cyk3 to the bud neck. Deletion of *HOF1* did not alter the timing of Cyk3 binding to the bud neck (data not shown). By contrast, the amount of Cyk3-GFP at the bud neck was strongly decreased in the majority of anaphase cells upon Inn1 depletion (supplementary material Fig. S5). Thus, the localization of Cyk3 to the bud neck depends upon Inn1 and MEN activity.

Primary-septum formation is compromised in MEN mutants

To better understand how the MEN contributes to cytokinesis, we analyzed the phenotype of MEN Gal1-*SIC1*^{S} mutants in greater detail. Inactivation of Cdk1 in arrested *dbf2-2 dbf20Δ* cells promoted spindle breakdown and nuclear division (data not shown). However, cells did not physically separate from each other, resulting in the accumulation of chains of interconnected cells (supplementary material Fig. S6). The bud-neck region of *dbf2-2 dbf20Δ* Gal1-*SIC1*^{S} cells was thus analyzed by high-resolution electron microscopy (Fig. 5). During cytokinesis, wild-type cells formed a normal primary septum, which appeared symmetrically from both sides of the sectioned bud neck. Symmetrical and bilateral extension of the primary septum inwards continued until it was completely closed (Fig. 5A1-A4). No septum formation was observed in arrested *dbf2-2 dbf20Δ* cells (Fig. 5B). In wild-type Gal1-*SIC1*^{S}-overexpressing cells, primary-septum extension was also centripetal but the septum appeared slightly thicker in comparison with wild-type cells (Fig. 5C1-C5). By marked contrast, *dbf2-2 dbf20Δ* Gal1-*SIC1*^{S} cells showed primary-septum growth mainly from one side of the bud neck (Fig. 5D1-D5). Asymmetric primary-septum formation covered the bud-neck area, producing curved or branching septa. Initiation of primary-septum extension from other foci was also observed after the initial septum was already extended (Fig. 6B4). It is therefore likely that, in MEN mutants with low Cdk1 activity, the speed of primary-septum extension varies along the bud-neck circumference, leading to asymmetric septum ingression. Furthermore, the timing of secondary-septum extension was abnormal in *dbf2-2 dbf20Δ* cells. In the wild type, with or without Sic1^{S} overproduction, the deposition of the secondary septum was first observed after the primary septum was already enclosed (Fig. 5A4,C4). However, primary- and secondary-septum extension occurred simultaneously in *dbf2-2 dbf20Δ* Gal1-*SIC1*^{S} cells (Fig. 5D1-D4). Thus, upon Cdk1 inactivation, MEN activity is important to promote centripetal (symmetric) primary-septum formation and to delay premature secondary-septum initiation.

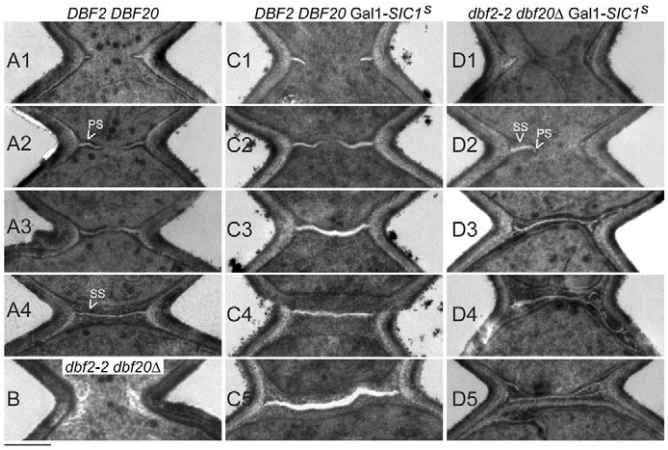

Fig. 5. Septum formation is compromised in MEN mutants. Electron micrographs of wild type (**A1-A4**), *dbf2-2 dbf20*Δ (**B**), Gal1-*SIC1*^{S} (**C1-C5**) and *dbf2-2 dbf20Δ* Gal1-*SIC1*^{S} (**D1-D5**) cells in late anaphase. Cells were treated as in Fig. 3. Several time points were analyzed after cell-cycle release in galactose containing medium at 37°C. PS, primary septum; SS, secondary septum. Scale bar: 0.5 μm.

Overexpression of *CYK3* abolishes the simultaneous extension of primary and secondary septa in MEN mutants

The localization data so far established that MEN activity is required to efficiently target Cyk3 to the bud neck. The abnormal

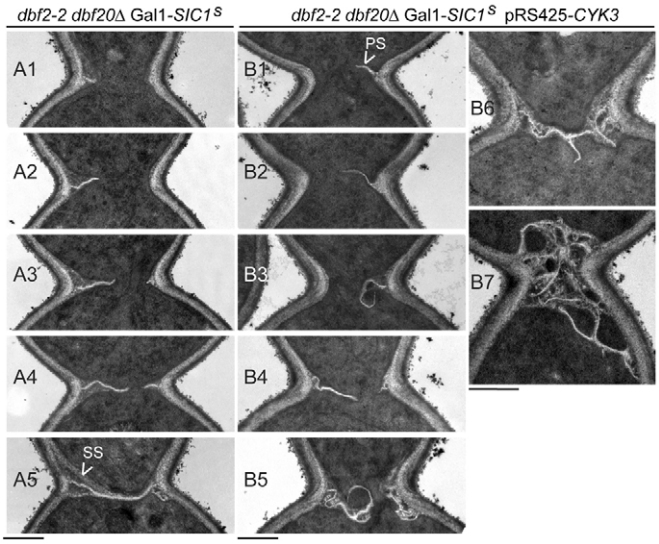

C

	PS - SS	PS + SS
dbf2-2 dbf20Δ Gal1-*SIC1*^{S}	17 %	83 %
dbf2-2 dbf20Δ Gal1-*SIC1*^{S} pRS425-*CYK3*	80 %	20 %

	symmetric	asymmetric
dbf2-2 dbf20Δ Gal1-*SIC1*^{S}	19 %	81 %
dbf2-2 dbf20Δ Gal1-*SIC1*^{S} pRS425-*CYK3*	35 %	65 %

Fig. 6. Overexpression of *CYK3* rescues the coordination of primary- and secondary-septum formation in MEN mutants. (**A**,**B**) Electron micrographs of late-anaphase cells of *dbf2-2 dbf20Δ* Gal1-*SIC1*^{S} (A1-A5) and *dbf2-2 dbf20Δ* Gal1-*SIC1*^{S} 2 μ-*CYK3* cells (B1-B7). Cell-cycle synchronization was performed as in Fig. 3. PS, primary septum; SS, secondary septum. (**C**) The following morphological phenotypes (A, *n*=53; B, *n*=40) were scored for: symmetric and asymmetric primary-septum extension, growing primary septum alone (PS-SS) or growing primary septum together with the secondary septa (PS+SS). Scale bars: 0.5 μm.

primary-septum formation observed in *dbf2-2 dbf20Δ* cells (Fig. 5) could therefore be a consequence of lower levels of Cyk3 at the bud neck in late mitosis. This notion was further supported by the fact that high *CYK3* gene dosage rescued the synthetic lethal interaction between MEN mutants and *myo1Δ*, *hof1Δ* and *inn1-ts* (data not shown), and led to the hypothesis that Cyk3 might work downstream of MEN in the actomyosin-independent pathway. Thus, using electron microscopy, we analyzed the phenotype of *dbf2-2 dbf20Δ* Gal1-*SIC1*^{S} cells carrying 2 μ-*CYK3* (high gene dosage). As shown before, primary-septum formation was asymmetric in most *dbf2-2 dbf20Δ* Gal1-*SIC1*^{S} cells (Fig. 6A1-A5). Overproduction of Cyk3 was unable to restore the symmetric primary-septum invagination but rather suppressed the simultaneous extension of the secondary and primary septa in *dbf2-2 dbf20Δ* Gal1-*SIC1*^{S} cells (Fig. 6B1-B5). Increased branching points of the primary septum were observed in 71% of the inspected cells (*n*=90; Fig. 6B6,B7). These data imply that Cyk3 overproduction has an inhibitory influence upon secondary-septum extension in *dbf2-2 dbf20Δ* cells in the presence of low Cdk1 activity.

Chs2 binds inefficiently to the bud neck in the absence of Dbf2/20 kinase activity

Because asymmetric primary-septum extension persisted in MEN mutants upon Cyk3 overproduction, we investigated whether localization of the enzyme Chs2, which synthesizes the primary septum at the bud neck (Cabib, 2004), is impaired in MEN mutants forced to exit mitosis by *SIC1*^{S} overexpression. Although Chs2 had been previously reported to localize at the bud neck in MEN mutants (Zhang et al., 2006), the amount of Chs2 targeted to the bud neck was never quantified.

Cdk1 sequesters Chs2 in the endoplasmic reticulum (ER) (Teh et al., 2009). After inactivation of Cdk1, the COPII secretory pathway transports Chs2 to the bud neck (Zhang et al., 2006). Consequently, in wild-type cells, Chs2-GFP localized in vesicles (Fig. 7A, arrowhead) and at the bud-neck region (Fig. 7A, asterisk). By contrast, in *dbf2-2 dbf20Δ* Gal1-*SIC1*^{S} cells, Chs2-GFP also accumulated at the bud neck but in a smaller percentage of cells and at later time points (Fig. 7C). Furthermore, vesicle-like staining was reduced in the mutant cells (Fig. 7A,C, arrowheads) and lower relative fluorescence intensity of Chs2-GFP at the bud-neck region was detected (Fig. 7D). Total Chs2 protein levels were, however, comparable between wild type and mutant (Fig. 7E), suggesting that changes in protein stability did not account for the reduced GFP signal at the bud neck in *dbf2-2 dbf20Δ* Gal1-*SIC1*^{S} cells.

We also analyzed the localization of Chs2 in *cyk3Δ* cells and observed no significant difference in comparison with the wild-type cells (data not shown). It is therefore unlikely that the reduced binding of Chs2-GFP at the bud neck in *dbf2-2 dbf20Δ* Gal1-*SIC1*^{S} cells is a consequence of loss of Cyk3 function. Moreover, Chs2 localization has been reported to be dependent upon proper splitting of the septin collar into two well-separated rings in late anaphase (Dobbelaere and Barral, 2004). However, septin-ring splitting was observed in *dbf2-2 dbf20Δ* Gal1-*SIC1*^{S} cells forced to exit mitosis, excluding this possibility (supplementary material Fig. S7).

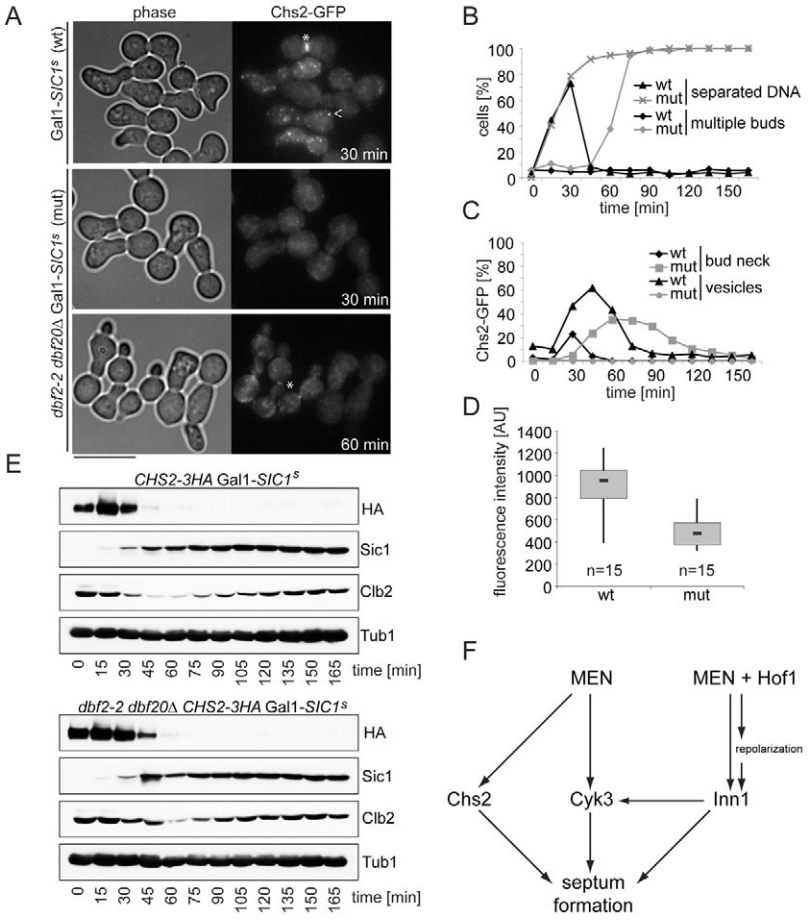

Fig. 7. Chs2 bud-neck accumulation is reduced in MEN mutants. (**A-D**) Chs2-GFP localization in Gal1-*SIC1*^{S} and *dbf2-2 dbf20Δ* Gal1-*SIC1*^{S} cells. The indicated cell types carrying *CHS2-GFP* were treated as in Fig. 3. Chs2-GFP bud-neck signal (A) and cell-cycle progression (B) were monitored over time. (C) Percentage of cells with dot-like Chs2-GFP staining (vesicles) and Chs2-GFP at the bud neck over time. In B and C, 100 cells were scored per time point. (D) Quantification of Chs2-GFP bud-neck signals in arbitrary units. (**E**) A similar experiment as in A was carried out for cells expressing *CHS2-3HA*. Protein levels of Chs2-3HA, Sic1, Clb2 and Tub1 (loading control) are shown for *CHS2-3HA* Gal1-*SIC1*^{S} and *CHS2-3HA dbf2-2 dbf20Δ* Gal1-*SIC1*^{S} cells. (**F**) Summary of the role of the MEN in Inn1, Cyk3 and Chs2 localization. MEN activity and Hof1 are required for targeted Inn1 bud-neck localization. Cyk3 bud-neck targeting depends upon MEN activity and Inn1. Chs2 is also under MEN control, because Chs2 did not efficiently accumulate at the bud neck in MEN mutants upon mitotic exit. Scale bar: 10 μm.

Collectively, these data demonstrate that accumulation of Chs2 at the bud neck is under the control of the MEN.

Discussion

Over the past decade, most of the studies regarding MEN signaling focused on the role of MEN in controlling the localization and activation of the phosphatase Cdc14 (Stegmeier and Amon, 2004). Although it is known that MEN components translocate to the site of cell division in late anaphase, the molecular role of MEN in cytokinesis is still ill defined (Balasubramanian et al., 2004; Surana et al., 1993). Our genetic data now show that the MEN is involved in multiple regulatory steps during cytokinesis. We found that MEN mutants were unable to survive in the absence of *MYO1*, *HOF1*, *CYK3* or functional *INN1*. These data extend previous studies reporting synthetic lethal interactions between MEN and the yeast IQGAP ortholog Iqg1, which is involved in both actomyosin-ring-dependent and -independent pathways and functions upstream of *HOF1* and *CYK3* (Corbett et al., 2006).

On the basis of genetic and functional analysis, we separated the function of the MEN in cytokinesis as depicted in Fig. 7F. MEN activity and Hof1 are important to relocate Inn1 to the bud neck, whereas impairment of only the MEN or *HOF1* did not interfere with the timing of Inn1 bud-neck localization. This localization defect of Inn1 in the absence of Hof1 was directly caused by MEN malfunction and was not the result of high Cdk1 activity. Thus, overlapping mechanisms involving MEN and Hof1 ensure Inn1 bud-neck association. Furthermore, we identified Cyk3 as an additional component that is directly regulated by the MEN after mitotic exit (Fig. 3). Cyk3 failed to bind to the bud neck in MEN mutants upon *SIC1* overexpression or direct Cdk1 inactivation. This defect was specific to Cyk3, because, under the same experimental conditions, Inn1 and Hof1 colocalized with the actomyosin-ring component Myo1. The reduced binding of Cyk3 to the bud neck in MEN mutants explains why those mutants are inviable in *myo1Δ*, *hof1Δ* and *inn1-ts* backgrounds. Consistently, increased levels of *CYK3* partially rescued the growth lethality of *dbf2-2 myo1Δ*, *dbf2-2 dbf20Δ hof1Δ* and *mob1-67 inn1-ts* cells (our unpublished data).

How MEN controls the localization of Cyk3 and Inn1 at the molecular level is still unclear. Interestingly, association of Cyk3 with the bud neck was drastically reduced upon Inn1 depletion, but it was unaltered in *hof1Δ* cells (supplementary material Fig. S5) (our unpublished observation). Thus, it is possible that MEN activity at the bud neck is involved in stabilization of the Inn1-Cyk3 interactions. Cyk3 is phosphorylated in vivo (Bodenmiller et al., 2008). So far, we were unable to show that Cyk3 is phosphorylated by MEN kinases using the criteria of a mobility shift on protein gels. Further analysis is necessary to establish whether Cyk3 is subjected to cell-cycle-dependent phosphorylation and whether MEN kinases are directly involved in this process. Inn1 is a phosphoprotein that is subject to cell-cycle-dependent phosphorylation (Nishihama et al., 2009). Hyperphosphorylation of Inn1 coincides with the time of its accumulation at the bud neck. However, although hyperphosphorylation of Inn1 is completely blocked by high mitotic Cdk1 activity, Inn1 is still hyperphosphorylated in *cdc15-1*, *cdc5-10* and *dbf2-2 dbf20Δ* cells forced to exit mitosis (Fig. 3 and our unpublished data). It is therefore likely that kinases other than Cdc15, Cdc5 and Dbf2/20 are involved in Inn1 regulation. Interestingly, Inn1 phosphorylation was completely blocked in *cdc15-1 hof1Δ* cells (but not in the single *cdc15-1* or *hof1Δ* mutants), in which Inn1 failed to localize to the bud neck (Fig. 3). It is thus tempting to speculate that Inn1 phosphorylation is executed by a bud-neck-associated kinase. Identification of Inn1-interacting kinases will be crucial to understand the role of phosphorylation in its function.

What are the functional consequences of loss of MEN activity for cytokinesis? Previous studies suggested a role of the MEN in septation, mainly based on the analysis of chitin staining in *cdc15-1* cells (Hwa Lim et al., 2003). We now show that *dbf2-2 dbf20Δ* cells were able to initiate septum formation upon Cdk1 inactivation, yet chitin deposition seemed reduced in these mutants in comparison with Gal1-*SIC1* wild-type cells (Fig. 5). Strikingly, extensions of the primary and secondary septa were mainly asymmetric and uncoordinated in *dbf2-2 dbf20Δ* cells. This defect drew our attention to the enzyme Chs2, which drives chitin deposition, a process that is necessary for the synthesis of the primary septum (Cabib, 2004). Chs2 is retained in the ER by the activity of mitotic Cdk1 and it is transported to the bud-neck region via COPII secretory vesicles upon mitotic exit (Zhang et al., 2006). Investigation of Chs2 localization in *dbf2-2 dbf20Δ* cells upon *SIC1* overexpression showed that, although Chs2 localized at the bud neck, the amount of Chs2 enriched at this location was drastically reduced, which is in line with the reduced chitin deposition observed in *dbf2-2 dbf20Δ* Gal1-*SIC1* cells. This defect could not be explained by lack of Cyk3 at the bud neck in MEN mutants, because Chs2 localization was identical in *cyk3Δ* and wild-type cells. Furthermore, it is unlikely that the absence of bud-neck-localized Cyk3 was the determinant of the asymmetric primary-septum extension in MEN mutants, because increased levels of *CYK3* did not rescue the asymmetric primary-septum extension of *dbf2-2 dbf20Δ* Gal1-*SIC1* cells (Fig. 6) and primary-septum extension was mainly symmetric in the *cyk3Δ* genetic background analyzed by electron microscopy (our unpublished observation). Because the appearance of Chs2-GFP-labeled vesicles was also strongly reduced in *dbf2-2 dbf20Δ* Gal1-*SIC1* mutants, it is possible that MEN affects vesicle transport at an early stage.

Contraction of the actomyosin ring and formation of the primary septum were reported to be interdependent processes (Schmidt et al., 2002). It is therefore possible that, upon mitotic exit, bud-neck-associated MEN activity triggers actomyosin-ring contraction, which in turn facilitates the docking and full activation of Chs2 to the bud neck. Alternatively, MEN activity could be required to promote the proper transport and activation of Chs2 to the bud neck, and active Chs2 could then promote actomyosin-ring contraction. So far, the molecular mechanisms leading to activation of Chs2 at the bud neck are unknown. Also, how the MEN regulates actomyosin-ring contraction at the molecular level is not understood. Identification of additional MEN targets at the bud neck will be essential not only to understand how actomyosin-ring contraction is regulated but also how actomyosin-dependent and -independent mechanisms are coordinated by the MEN.

In budding yeast, the bilateral deposition of the secondary septum occurs after completion of the primary septum (Cabib et al., 1982). How these two processes are coordinated is still unclear. Our electron-microscopic analysis showed that primary and secondary septa simultaneously extended after mitotic exit in cells deficient in both *dbf2* and *dbf20*. Interestingly, overproduction of Cyk3 was able to suppress premature secondary-septum deposition in *dbf2-2 dbf20Δ* Gal1-*SIC1* cells. Although no direct link has been established between Cyk3 and components involved in secondary-septum extension, our data suggest that the MEN could

be directly involved in regulating the timely coordination of formation of primary and secondary septa via Cyk3.

Cytokinesis defects related to septum formation and localization of the bud-neck components Inn1, Cyk3 and Chs2 were observed for a range of MEN mutants. Also, inactivation of Cdc14 phosphatase, which is the ultimate target of the MEN and directly involved in mitotic Cdk1 inactivation, caused similar phenotypes. Because Cdc14 is not active in MEN mutants forced to exit mitosis upon *SIC1* overexpression, and positive-feedback mechanisms involving Cdc14 are important for MEN activation (Jaspersen and Morgan, 2000; Konig et al., 2010; Shou et al., 1999; Visintin et al., 1999), we are presently unable to differentiate the individual contribution of MEN kinases and Cdc14 for the specific phenotypes using our current experimental approach. Future investigations should therefore concentrate on the establishment of separation-of-function mutants to evaluate the contribution of each MEN component during cytokinesis.

In budding yeast and other eukaryotes, cytokinesis will not start until the activity of the mitotic Cdk1 is downregulated (Balasubramanian et al., 2004). In this way, cells ensure that all events required for chromosome segregation, which are mainly regulated by Cdk1-dependent phosphorylation, are completed prior to the division of the cytoplasm. We propose that the MEN has a fundamental role in the coordination of cytokinesis in budding yeast by bringing together components involved in actomyosin-ring contraction and septum formation after mitotic exit. In fission yeast, the septation initiation network (SIN) predominantly regulates cytokinesis rather than mitotic exit (Krapp and Simanis, 2008; McCollum and Gould, 2001). SIN components are involved in triggering medial ring constriction and septum formation (Roberts-Galbraith and Gould, 2008). Considering the high similarity between MEN and SIN kinases, it is possible that MEN and SIN might share common substrates involved in septation and/or cytokinesis. Identification of MEN and/or SIN substrates will be fundamental to understand the molecular mechanisms that coordinate cytokinesis with mitotic exit.

Materials and Methods

Strains, plasmids, growth conditions and genetic methods

Yeast strains and plasmids used in this study are described in supplementary material Tables S1 and S2. Yeast growth conditions and media were as described (Sherman, 1991). Gene deletions and epitope tagging were performed using PCR-based methods (Janke et al., 2004; Knop et al., 1999). *Td-inn1* cells were constructed and grown as described (Sanchez-Diaz et al., 2008). Yeast strains were grown in yeast peptone dextrose medium containing 0.1 mg/l adenine (YPAD). Instead of dextrose, either 3% raffinose (YPAR) or a mixture of 3% raffinose and 2% galactose (YPARG) were used in experiments involving expression of genes under control of the Gal1 promoter. Synthetic complete (SC) media were used to grow strains bearing plasmids. To test for loss of *URA3*-containing plasmids, 1 mg/ml 5′flurоorotic acid (5′FOA) was added to the plates. To induce G1-phase arrest, cells were incubated with 10 μg/ml synthetic α-factor (Sigma) for 1.5 generation cycles. When appropriate, cells were blocked in metaphase by washing α-factor-arrested cells in medium containing 1.5 μg/ml nocodazole (Sigma). For Cdk1 inhibition, *cdk1-as1* cells were treated with 0.5 μM of 1NM-PP1 (Sigma) as described (Bishop et al., 2000).

Protein methods

Yeast protein extracts and western blotting were performed as described (Janke et al., 2004). Antibodies were rabbit anti-GFP antibody (gift from Elmar Schiebel, University of Heidelberg, Germany), mouse anti-tubulin (Tub1; gift from E. Schiebel), mouse anti-HA (clone 12CA5, Sigma) rabbit anti-Clb2 and guinea-pig anti-Sic1 (Maekawa et al., 2007). Secondary antibodies were goat anti-mouse, goat anti-rabbit and goat anti-guinea-pig IgGs coupled to horseradish peroxidase (Jackson ImmunoResearch Laboratories).

Microscopic techniques

For fluorescence microscopy, 1.3 μl of each cell culture was spotted onto microscope slides and immediately inspected. Cells were fixed with 70% ethanol and resuspended in PBS containing 1 μg/ml 4′,6-diamino-2-phenylindole (DAPI, Sigma) whenever DNA visualization was needed. Cells carrying GFP or Cherry fusion proteins were fixed in 4% formaldehyde for 10-30 minutes before inspection. For actin staining, 1 volume of 3.7% formaldehyde was immediately added to 10 volumes of cell culture. After an incubation of 10 minutes, cells were resuspended in fresh 3.7% formaldehyde solution in PBS and incubated for 60 minutes. Actin was stained with 2 μM Rhodamine-phalloidin (Invitrogen). For live-cell imaging, cells were adhered onto glass-bottomed Petri dishes (MatTek) using concanavalin A-Type IV (Sigma) as described (Caydasi and Pereira, 2009). A Zeiss Axiophot microscope equipped with a 100× NA 1.45 A Plan-Fluor oil-immersion objective (Zeiss), a Cascade 1K CCD camera (Photometrics) and MetaMorph software (Universal Imaging Corp.) was used for all experiments. Quantification of fluorescence intensity was performed using ImageJ software (NIH, Bethesda). The mean pixel intensities of bud-neck signals were determined using the plane with the strongest signal. Background signals were measured in the near proximity of the bud neck and subtracted from bud-neck measurements.

Cells were treated for electron microscopy accordingly to Maier et al. (Maier et al., 2008). Briefly, cells were fixed with 2.5% glutaraldehyde and 4% potassium permanganate for 30 minutes each. After incubation with aqueous saturated uranyl acetate for 30 minutes, cells were consecutively dehydrated using 30%, 50% and 100% ethanol solutions and imbedded in EPON-812 (Agar Scientific). Sections of 70 nm were analyzed using a Philips EM 410 microscope (FEI Eindhofen Netherlands) equipped with a Gatan BioScan 792 digital camera and DigitalMicrograph software (Gatan, Pleasanton, CA).

We thank Phil Hieter for the *inn1-ts* strain; Elmar Schiebel for antibodies; Michael Knop for sharing protocols; Astrid Hofmann for excellent technical assistance; Karsten Richter for support with electron microscopy; Elmar Schiebel, David Gillespie and Fouzia Ahmad for critical comments on the manuscript; and members of the G.P. laboratory for helpful discussions. F.M., B.P., I.M.L. and D.T.B. were funded by the Marie Curie Grant MEXT-CT-042544. I.M.L. is supported by the Hartmut Hoffmann-Berling International Graduate School (HBIGS). The work of G.P. is funded by the Marie Curie Grant MEXT-CT-042544 and Helmholtz Young Investigator Grant HZ-NG-111.

Supplementary material available online at
http://jcs.biologists.org/cgi/content/full/123/11/1851/DC1

References

Balasubramanian, M. K., Bi, E. and Glotzer, M. (2004). Comparative analysis of cytokinesis in budding yeast, fission yeast and animal cells. *Curr. Biol.* **14**, R806-R818.

Bardin, A. J. and Amon, A. (2001). Men and sin: what's the difference? *Nat. Rev. Mol. Cell Biol.* **2**, 815-826.

Bembenek, J., Kang, J., Kurischko, C., Li, B., Raab, J. R., Belanger, K. D., Luca, F. C. and Yu, H. (2005). Crm1-mediated nuclear export of Cdc14 is required for the completion of cytokinesis in budding yeast. *Cell Cycle* **4**, 961-971.

Ben-Aroya, S., Coombes, C., Kwok, T., O'Donnell, K. A., Boeke, J. D. and Hieter, P. (2008). Toward a comprehensive temperature-sensitive mutant repository of the essential genes of Saccharomyces cerevisiae. *Mol. Cell* **30**, 248-258.

Bi, E. (2001). Cytokinesis in budding yeast: the relationship between actomyosin ring function and septum formation. *Cell Struct. Funct.* **26**, 529-537.

Bi, E., Maddox, P., Lew, D. J., Salmon, E. D., McMillan, J. N., Yeh, E. and Pringle, J. R. (1998). Involvement of an actomyosin contractile ring in Saccharomyces cerevisiae cytokinesis. *J. Cell Biol.* **142**, 1301-1312.

Bishop, A. C., Ubersax, J. A., Petsch, D. T., Matheos, D. P., Gray, N. S., Blethrow, J., Shimizu, E., Tsien, J. Z., Schultz, P. G., Rose, M. D. et al. (2000). A chemical switch for inhibitor-sensitive alleles of any protein kinase. *Nature* **407**, 395-401.

Bodenmiller, B., Campbell, D., Gerrits, B., Lam, H., Jovanovic, M., Picotti, P., Schlapbach, R. and Aebersold, R. (2008). PhosphoPep-a database of protein phosphorylation sites in model organisms. *Nat. Biotechnol.* **26**, 1339-1340.

Cabib, E. (2004). The septation apparatus, a chitin-requiring machine in budding yeast. *Arch. Biochem. Biophys.* **426**, 201-207.

Cabib, E., Roberts, R. and Bowers, B. (1982). Synthesis of the yeast cell wall and its regulation. *Annu. Rev. Biochem.* **51**, 763-793.

Caydasi, A. K. and Pereira, G. (2009). Spindle alignment regulates the dynamic association of checkpoint proteins with yeast spindle pole bodies. *Dev. Cell* **16**, 146-156.

Christianson, T. W., Sikorski, R. S., Dante, M., Shero, J. H. and Hieter, P. (1992). Multifunctional yeast high-copy-number shuttle vectors. *Gene* **110**, 119-122.

Chuang, J. S. and Schekman, R. W. (1996). Differential trafficking and timed localization of two chitin synthase proteins, Chs2p and Chs3p. *J. Cell Biol.* **135**, 597-610.

Corbett, M., Xiong, Y., Boyne, J. R., Wright, D. J., Munro, E. and Price, C. (2006). IQGAP and mitotic exit network (MEN) proteins are required for cytokinesis and re-polarization of the actin cytoskeleton in the budding yeast, Saccharomyces cerevisiae. *Eur J. Cell Biol.* **85**, 1201-1215.

Dobbelaere, J. and Barral, Y. (2004). Spatial coordination of cytokinetic events by compartmentalization of the cell cortex. *Science* **305**, 393-396.
Epp, J. A. and Chant, J. (1997). An IQGAP-related protein controls actin-ring formation and cytokinesis in yeast. *Curr. Biol.* **7**, 921-929.
Frenz, L. M., Lee, S. E., Fesquet, D. and Johnston, L. H. (2000). The budding yeast Dbf2 protein kinase localises to the centrosome and moves to the bud neck in late mitosis. *J. Cell Sci.* **113**, 3399-3408.
Gietz, R. D. and Sugino, A. (1988). New yeast-Escherichia coli shuttle vectors constructed with in vitro mutagenized yeast genes lacking six-base pair restriction sites. *Gene* **74**, 527-534.
Guertin, D. A., Trautmann, S. and McCollum, D. (2002). Cytokinesis in eukaryotes. *Microbiol. Mol. Biol. Rev.* **66**, 155-178.
Hwa Lim, H., Yeong, F. M. and Surana, U. (2003). Inactivation of mitotic kinase triggers translocation of MEN components to mother-daughter neck in yeast. *Mol. Biol. Cell* **14**, 4734-4743.
Janke, C., Magiera, M. M., Rathfelder, N., Taxis, C., Reber, S., Maekawa, H., Moreno-Borchart, A., Doenges, G., Schwob, E., Schiebel, E. et al. (2004). A versatile toolbox for PCR-based tagging of yeast genes: new fluorescent proteins, more markers and promoter substitution cassettes. *Yeast* **21**, 947-962.
Jaspersen, S. L. and Morgan, D. O. (2000). Cdc14 activates cdc15 to promote mitotic exit in budding yeast. *Curr. Biol.* **10**, 615-618.
Kamei, T., Tanaka, K., Hihara, T., Umikawa, M., Imamura, H., Kikyo, M., Ozaki, K. and Takai, Y. (1998). Interaction of Bnr1p with a novel Src homology 3 domain-containing Hof1p. Implication in cytokinesis in Saccharomyces cerevisiae. *J. Biol. Chem.* **273**, 28341-28345.
Knop, M., Siegers, K., Pereira, G., Zachariae, W., Winsor, B., Nasmyth, K. and Schiebel, E. (1999). Epitope tagging of yeast genes using a PCR-based strategy: more tags and improved practical routines. *Yeast* **15**, 963-972.
Konig, C., Maekawa, H. and Schiebel, E. (2010). Mutual regulation of cyclin-dependent kinase and the mitotic exit network. *J. Cell Biol.* **188**, 351-368.
Korinek, W. S., Bi, E., Epp, J. A., Wang, L., Ho, J. and Chant, J. (2000). Cyk3, a novel SH3-domain protein, affects cytokinesis in yeast. *Curr. Biol.* **10**, 947-950.
Krapp, A. and Simanis, V. (2008). An overview of the fission yeast septation initiation network (SIN). *Biochem. Soc. Trans.* **36**, 411-415.
Lew, D. J. and Reed, S. I. (1993). Morphogenesis in the yeast cell cycle: regulation by Cdc28 and cyclins. *J. Cell Biol.* **120**, 1305-1320.
Lippincott, J. and Li, R. (1998a). Dual function of Cyk2, a cdc15/PSTPIP family protein, in regulating actomyosin ring dynamics and septin distribution. *J. Cell Biol.* **143**, 1947-1960.
Lippincott, J. and Li, R. (1998b). Sequential assembly of myosin II, an IQGAP-like protein, and filamentous actin to a ring structure involved in budding yeast cytokinesis. *J. Cell Biol.* **140**, 355-366.
Luca, F. C., Mody, M., Kurischko, C., Roof, D. M., Giddings, T. H. and Winey, M. (2001). Saccharomyces cerevisiae Mob1p is required for cytokinesis and mitotic exit. *Mol. Cell. Biol.* **21**, 6972-6983.
Maeder, C. I., Hink, M. A., Kinkhabwala, A., Mayr, R., Bastiaens, P. I. and Knop, M. (2007). Spatial regulation of Fus3 MAP kinase activity through a reaction-diffusion mechanism in yeast pheromone signalling. *Nat. Cell. Biol.* **9**, 1319-1326.
Maekawa, H., Priest, C., Lechner, J., Pereira, G. and Schiebel, E. (2007). The yeast centrosome translates the positional information of the anaphase spindle into a cell cycle signal. *J. Cell Biol.* **179**, 423-436.
Maier, P., Rathfelder, N., Maeder, C. I., Colombelli, J., Stelzer, E. H. and Knop, M. (2008). The SpoMBe pathway drives membrane bending necessary for cytokinesis and spore formation in yeast meiosis. *EMBO J.* **27**, 2363-2374.
McCollum, D. and Gould, K. L. (2001). Timing is everything: regulation of mitotic exit and cytokinesis by the MEN and SIN. *Trends Cell. Biol.* **11**, 89-95.
Moseley, J. B. and Goode, B. L. (2006). The yeast actin cytoskeleton: from cellular function to biochemical mechanism. *Microbiol. Mol. Biol. Rev.* **70**, 605-645.
Nasmyth, K. (1993). Control of the yeast cell cycle by the Cdc28 protein kinase. *Curr. Opin. Cell Biol.* **5**, 166-179.
Nishihama, R., Schreiter, J. H., Onishi, M., Vallen, E. A., Hanna, J., Moravcevic, K., Lippincott, M. F., Han, H., Lemmon, M. A., Pringle, J. R. et al. (2009). Role of Inn1 and its interactions with Hof1 and Cyk3 in promoting cleavage furrow and septum formation in S. cerevisiae. *J. Cell Biol.* **185**, 995-1012.
Pereira, G. and Schiebel, E. (2001). The role of the yeast spindle pole body and the mammalian centrosome in regulating late mitotic events. *Curr. Opin. Cell Biol.* **13**, 762-769.
Pereira, G., Manson, C., Grindlay, J. and Schiebel, E. (2002). Regulation of the Bfa1p-Bub2p complex at spindle pole bodies by the cell cycle phosphatase Cdc14p. *J. Cell Biol.* **157**, 367-379.
Roberts-Galbraith, R. H. and Gould, K. L. (2008). Stepping into the ring: the SIN takes on contractile ring assembly. *Genes Dev.* **22**, 3082-3088.
Rodriguez, J. R. and Paterson, B. M. (1990). Yeast myosin heavy chain mutant: maintenance of the cell type specific budding pattern and the normal deposition of chitin and cell wall components requires an intact myosin heavy chain gene. *Cell Motil. Cytoskeleton* **17**, 301-308.
Sanchez-Diaz, A., Marchesi, V., Murray, S., Jones, R., Pereira, G., Edmondson, R., Allen, T. and Labib, K. (2008). Inn1 couples contraction of the actomyosin ring to membrane ingression during cytokinesis in budding yeast. *Nat. Cell Biol.* **10**, 395-406.
Sburlati, A. and Cabib, E. (1986). Chitin synthetase 2, a presumptive participant in septum formation in Saccharomyces cerevisiae. *J. Biol. Chem.* **261**, 15147-15152.
Schmidt, M., Bowers, B., Varma, A., Roh, D. H. and Cabib, E. (2002). In budding yeast, contraction of the actomyosin ring and formation of the primary septum at cytokinesis depend on each other. *J. Cell Sci.* **115**, 293-302.
Schwob, E., Bohm, T., Mendenhall, M. D. and Nasmyth, K. (1994). The B-type cyclin kinase inhibitor p40SIC1 controls the G1 to S transition in S. cerevisiae. *Cell* **79**, 233-244.
Shannon, K. B. and Li, R. (1999). The multiple roles of Cyk1p in the assembly and function of the actomyosin ring in budding yeast. *Mol. Biol. Cell* **10**, 283-296.
Sherman, F. (1991). Getting started with yeast. *Methods Enzymol.* **194**, 3-21.
Shou, W., Seol, J. H., Shevchenko, A., Baskerville, C., Moazed, D., Chen, Z. W., Jang, J., Shevchenko, A., Charbonneau, H. and Deshaies, R. J. (1999). Exit from mitosis is triggered by Tem1-dependent release of the protein phosphatase Cdc14 from nucleolar RENT complex. *Cell* **97**, 233-244.
Sikorski, R. S. and Hieter, P. (1989). A system of shuttle vectors and yeast host strains designed for efficient manipulation of DNA in Saccharomyces cerevisiae. *Genetics* **122**, 19-27.
Song, S., Grenfell, T. Z., Garfield, S., Erikson, R. L. and Lee, K. S. (2000). Essential function of the polo box of Cdc5 in subcellular localization and induction of cytokinetic structures. *Mol. Cell. Biol.* **20**, 286-298.
Stegmeier, F. and Amon, A. (2004). Closing mitosis: the functions of the Cdc14 phosphatase and its regulation. *Annu. Rev. Genet.* **38**, 203-232.
Surana, U., Amon, A., Dowzer, C., McGrew, J., Byers, B. and Nasmyth, K. (1993). Destruction of the CDC28/CLB mitotic kinase is not required for the metaphase to anaphase transition in budding yeast. *EMBO J.* **12**, 1969-1978.
Taxis, C. and Knop, M. (2006). System of centromeric, episomal, and integrative vectors based on drug resistance markers for Saccharomyces cerevisiae. *Biotechniques* **40**, 73-78.
Teh, E. M., Chai, C. C. and Yeong, F. M. (2009). Retention of Chs2p in the ER requires N-terminal CDK1-phosphorylation sites. *Cell Cycle* **8**, 2964-2974.
Vallen, E. A., Caviston, J. and Bi, E. (2000). Roles of Hof1p, Bni1p, Bnr1p, and myo1p in cytokinesis in Saccharomyces cerevisiae. *Mol. Biol. Cell* **11**, 593-611.
Visintin, R., Hwang, E. S. and Amon, A. (1999). Cfi1 prevents premature exit from mitosis by anchoring Cdc14 phosphatase in the nucleolus. *Nature* **398**, 818-823.
Watts, F. Z., Shiels, G. and Orr, E. (1987). The yeast MYO1 gene encoding a myosin-like protein required for cell division. *EMBO J* **6**, 3499-3505.
Wiedenmann, J., Schenk, A., Rocker, C., Girod, A., Spindler, K. D. and Nienhaus, G. U. (2002). A far-red fluorescent protein with fast maturation and reduced oligomerization tendency from Entacmaea quadricolor (Anthozoa, Actinaria). *Proc. Natl. Acad. Sci. USA* **99**, 11646-11651.
Xu, S., Huang, H. K., Kaiser, P., Latterich, M. and Hunter, T. (2000). Phosphorylation and spindle pole body localization of the Cdc15p mitotic regulatory protein kinase in budding yeast. *Curr. Biol.* **10**, 329-332.
Yeong, F. M. (2005). Severing all ties between mother and daughter: cell separation in budding yeast. *Mol. Microbiol.* **55**, 1325-1331.
Yeong, F. M., Lim, H. H. and Surana, U. (2002). MEN, destruction and separation: mechanistic links between mitotic exit and cytokinesis in budding yeast. *BioEssays* **24**, 659-666.
Yoshida, S., Kono, K., Lowery, D. M., Bartolini, S., Yaffe, M. B., Ohya, Y. and Pellman, D. (2006). Polo-like kinase Cdc5 controls the local activation of Rho1 to promote cytokinesis. *Science* **313**, 108-111.
Zhang, G., Kashimshetty, R., Ng, K. E., Tan, H. B. and Yeong, F. M. (2006). Exit from mitosis triggers Chs2p transport from the endoplasmic reticulum to mother-daughter neck via the secretory pathway in budding yeast. *J. Cell Biol.* **174**, 207-220.